Progress in Nuclear Science and Technology
Volume 8 (2025) pp. 286-290

DOI: 10.15669/pnst.8.286

ARTICLE

A Simple Process Simulation Method for Radiation Stability Evaluation of Minor Actinides Separation

Tomohiro TOIGAWA*, Yasuhiro TSUBATA , Yuta KUMAGAI and Yasutoshi BAN

Japan Atomic Energy Agency, 2-4 Shirakata, Tokai-mura, Naka-gun, Ibaraki-ken, 319-1195, Japan

We propose a simple process simulation methodology that uses readily available information about radiation impact. The process simulation was conducted for a minor actinides (MA) separation process while considering the degradation of extraction ability by radiolysis. The simulation provided a processing limit of MA and enabled the evaluation of radiation stability.

KEYWORDS: MA separation process, radiation stability, solvent extraction, TDdDGA, process simulation

I. Introduction

The radiation stability of the extraction solvent for minor actinides (MA) separation is a critical requirement for the safety and efficient operation of the MA separation process. The radiation stability of the extraction solvent has been investigated through experimental methods involving radioisotopes and charged particle accelerators.[1-7] These studies have provided valuable information on the degradation of the extraction ability,[2,3] the radiation chemical yields known as the G-values,[4,5] and the rate constants for related radiation-chemical reactions of extractants with the radiolysis products.[6,7] The radiation-chemical reactions in extraction-solvent and resulting radiolysis products are enormously diverse because the primary radiolysis products are highly oxidative/reductive species. Therefore, it is still challenging to incorporate all radiation-chemical reactions into the process simulations in detail.

Herein, we propose a process simulation methodology simply introducing an experimentally determined dose-dependent distribution ratio to evaluate the radiation stability. This methodology was demonstrated in an extraction process for recovering MA and rare earths from high-level liquid waste (HLLW) using *N,N,N′,N′*-tetradodecyldiglycolamide (TDdDGA) as an extractant. TDdDGA is one of the promising extractants for this process due to its high extraction capacity for MA and rare earth. Thus TDdDGA plays a crucial role in the so-called SELECT process developed by the Japan Atomic Energy Agency, to recover these elements.[8] Although the SELECT process has subsequent steps to purify MA using other extractants such as *N,N,N′,N′,N″,N″*-hexaoctyl nitrilotriacetamide[9] and alkyl diamidoamine with 2-ethylhexyl alkyl chains,[10] TDdDGA is expected to receive more radiation energy than those extractants used in the latter steps. Therefore, we focused on the TDdDGA process for the demonstration.

II. Methods

1. Targeted Process

The organic phase in the TDdDGA process consisted of 0.1 mol/dm^3 TDdDGA diluted by *n*-dodecane containing 20 vol.% 2-ethyl-1-hexanol (2-Et-1-HexOH). For extraction and separation of MA, the aqueous feed solution contains 1.5 mol/dm^3 nitric acid, 0.02 mol/dm^3 *N*-(2-hydroxyethyl)ethylenediamine-*N,N′,N′*-triacetic acid (HEDTA), and 0.1 mol/dm^3 hydrogen peroxide. A scrub solution was used to scrub some of fission products; it also contains same nitric acid, HEDTA and hydrogen peroxide concentration. For stripping MA and rare earth, 0.02 mol/dm^3 nitric acid aqueous solution is used.

A flowsheet for TDdDGA process considered here is shown in **Fig. 1**. The extraction apparatus has 32 stages of mixer-settler units and consists of 3 parts: 6 stages for extraction, 10 stages for scrub, and 16 stages for strip. The feed, scrub, and strip solution were fed into the 6th, 16th, and 32nd stages, respectively. The volume of each mixing part is 7.4 cm^3, while that of each settling part is 25 cm^3 except for 16th and 32nd stages, the last stages of the scrub and strip part, respectively, which have a volume of 41 cm^3. The structural dimension of the extraction apparatus was adopted as a model of an extraction apparatus used in our facility and was considered in the dose-estimation. The flow rates for each solution were also noted in Fig. 1. In this calculation, recycling of the organic phase was assumed as shown in Fig. 1, and the total organic phase volume was set to be 2910 cm^3. The volume of organic and aqueous phases in each mixing part were assumed to be the same; and the mixture form oil-in-water emulsion where the oil droplet has 100 μm diameter, which was chosen as a typical value based on the previous microscopic observation.[11] These assumptions were needed for dose estimation.

The main radionuclides in the feed solution considered

---

*Corresponding author, E-mail: toigawa.tomohiro@jaea.go.jp

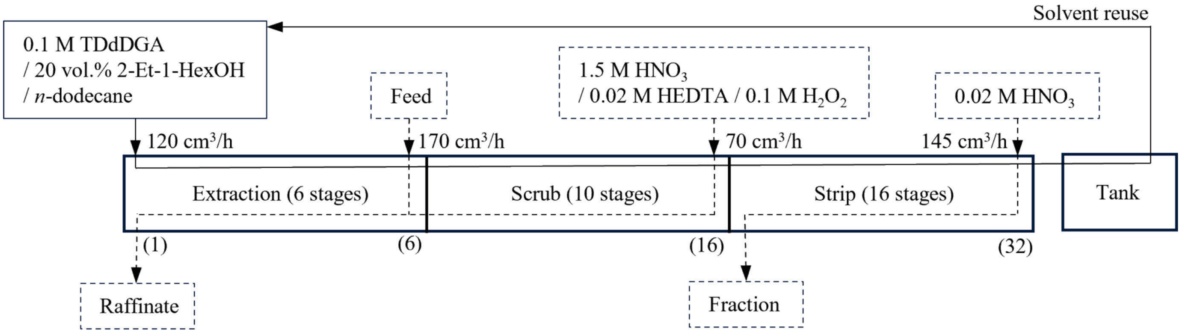

Fig. 1 Flowsheet of TDdDGA process. The solid lines and dashed lines represent the organic stream and the aqueous stream, respectively. The numbers in parentheses are stage numbers.

here are tabulated in **Table 1**. The radioactivity for each radionuclide was taken from the assay of a liquid waste stored in our facility. It was assumed that the concentrations of all the constituents are sufficiently low compared to the extraction capacity of the organic phase.

Table 1 Radioactivity (*A*) composition in the feed solution

Nuclide	A / Bq cm^{-3}
^{90}Sr	7.13×10^7
^{90}Y	7.13×10^7
^{137}Cs	1.59×10^8
^{137m}Ba	1.59×10^8
^{154}Eu	2.48×10^6
^{238}Pu	2.80×10^6
^{241}Am	1.07×10^7
^{244}Cm	1.84×10^7

2. Process Simulation

The mass-balance differential equation for a multistage counter-current mixer-settler extraction process [12] was solved numerically to obtain time-dependent behaviors of the constituents, including radionuclides. A dose-dependent distribution ratio, $D(x)$, was applied to consider the radiation impact, where x represents the effective absorbed dose. In our calculation, the stage efficiency was assumed to be 100% regardless of the radiation impact for simplification. The potential degradation of phase separation efficiency due to physical property changes such as increased viscosity is not considered in this model and remains as a subject for future investigation. Based on these assumptions, the mass-balance differential equations were described as follows;

$$\frac{d}{dt}C^p_{i,\mathrm{mix,org}} = \frac{D(x)F_{i,\mathrm{org}}C^p_{i,\mathrm{in,org}}+D(x)F_{i,\mathrm{aq}}C^p_{i,\mathrm{in,aq}}}{D(x)V_{i,\mathrm{mix,org}}+V_{i,\mathrm{mix,aq}}} - \frac{D(x)F_{i,\mathrm{org}}+F_{i,\mathrm{aq}}}{D(x)V_{i,\mathrm{mix,org}}+V_{i,\mathrm{mix,aq}}}C^p_{i,\mathrm{mix,org}}, \tag{1}$$

$$\frac{d}{dt}C^p_{i,\mathrm{mix,aq}} = \frac{F_{i,\mathrm{org}}C^p_{i,\mathrm{in,org}}+F_{i,\mathrm{aq}}C^p_{i,\mathrm{in,aq}}}{D(x)V_{i,\mathrm{mix,org}}+V_{i,\mathrm{mix,aq}}} - \frac{D(x)F_{i,\mathrm{org}}+F_{i,\mathrm{aq}}}{D(x)V_{i,\mathrm{mix,org}}+V_{i,\mathrm{mix,aq}}}C^p_{i,\mathrm{mix,aq}}, \tag{2}$$

$$\frac{d}{dt}C^p_{i,\mathrm{set,org}} = \frac{F_{i,\mathrm{org}}}{V_{i,\mathrm{set,org}}}C^p_{i,\mathrm{mix,org}} - \frac{F_{i,\mathrm{org}}}{V_{i,\mathrm{set,org}}}C^p_{i,\mathrm{set,org}}, \tag{3}$$

$$\frac{d}{dt}C^p_{i,\mathrm{set,aq}} = \frac{F_{i,\mathrm{aq}}}{V_{i,\mathrm{set,aq}}}C^p_{i,\mathrm{mix,aq}} - \frac{F_{i,\mathrm{aq}}}{V_{i,\mathrm{set,aq}}}C^p_{i,\mathrm{set,aq}}, \tag{4}$$

where $C^p_{i,part,phase}$ represents the concentration of a constituent or a radionuclide, p, in the ith stage mixier/settler part ($part$ = mix or set) organic/aqueous phase ($phase$ = org or aq); $F_{i,phase}$ is the flow rate for each phase in ith stage, which satisfy the following equations;

$$F_{i,\mathrm{org}} = F_{i-1,\mathrm{org}}, \tag{5}$$

$$F_{i,\mathrm{aq}} = \eta_{i,\mathrm{aq}}F_{i+1,\mathrm{aq}} + F_{i,\mathrm{feed,aq}}, \tag{6}$$

where $\eta_{i,\mathrm{aq}}$ represents the proportion of inflow to the ith stage from the upstream. If the aqueous phase in previous stage flows out form the mixer-settler system as raffinate or fraction, $\eta_{i,\mathrm{aq}} = 0$; otherwise $\eta_{i,\mathrm{aq}} = 1$. $F_{i,\mathrm{feed,aq}}$ is the flow rate of external feed; $V_{i,part,phase}$ is the volume of aqueous or organic phase in each part and stage; $C^p_{i,\mathrm{in},phase}$ represents the concentration in the inflow solution obtained from following equations;

$$C^p_{i,\mathrm{in,org}} = \frac{F_{i-1,\mathrm{org}}C^p_{i-1,\mathrm{set,org}}}{F_{i,\mathrm{org}}}, \tag{7}$$

$$C^p_{i,\mathrm{in,aq}} = \frac{\eta_{i,\mathrm{aq}}F_{i+1,\mathrm{aq}}C^p_{i+1,\mathrm{set,aq}}+F_{i,\mathrm{feed,aq}}C^p_{i,\mathrm{feed,aq}}}{F_{i,\mathrm{org}}}, \tag{8}$$

where $C^p_{i,\mathrm{feed,aq}}$ corresponds to the concentration in the external feed solution.

The dose rate was estimated according to the distribution of the radionuclides with the aid of a Monte-Carlo-based Particle and Heavy Ion Transport code System (PHITS) [13] to consider the radiation transport in the mixer-settler system. Radiation type (i.e., alpha, beta, and gamma radiations) and its initial kinetic energy from the radionuclides listed in Table 1 were referred from the RI-source function equipped in PHITS code. In the calculation of the dose rate of a certain stage, contributions from the radionuclides contained in the surrounding mixer or settler units were taken into consideration, in addition to those contained in itself. Since the extraction solvent continuously flows and circulates in the mixer-settler system, it is necessary to define an effective absorbed dose when two solvents mix. We estimated the effective dose as the volume average when the organic phase flows out to the next stage or in from the previous stage. The effective dose, x, for each stage and given time was formulated in a manner similar to the mass-balance differential equation, as follows;

$$\frac{d}{dt}x_{i,\mathrm{mix}} = \frac{F_{i,\mathrm{org}}}{V_{i,\mathrm{mix,org}}}x_{i-1,\mathrm{set}} - \frac{F_{i,\mathrm{org}}}{V_{i,\mathrm{mix,org}}}x_{i,\mathrm{mix}} + \sum_p \sum_j \sum_{part} \sum_{phase} a^p_{i,\mathrm{mix}|j,part,phase} A^p_{j,part,phase}, \tag{9}$$

$$\frac{d}{dt}x_{i,\mathrm{set}} = \frac{F_{i,\mathrm{org}}}{V_{i,\mathrm{set,org}}}x_{i,\mathrm{mix}} - \frac{F_{i,\mathrm{org}}}{V_{i,\mathrm{set,org}}}x_{i,\mathrm{set}} + \sum_p \sum_j \sum_{part} \sum_{phase} a^p_{i,\mathrm{set}|j,part,phase} A^p_{j,part,phase}, \tag{10}$$

where $x_{i,part}$ represents the effective dose for the mixier/settler part in the ith stage; $A^p_{i,part,phase}$ corresponds to the radioactivity concentration obtained from $\lambda^p C^p_{i,part,phase}$ where λ^p is the disintegration constant; a is a coefficient to express the inter-stage contributions in the dose from the surrounding stages and $a^p_{i,part|j,part',phase'}$ corresponds the dose from a radionuclide, p, dissolving in the mixier/settler part organic/aqueous phase in the jth stage, to extraction solvent in the mixier/settler part in the ith stage. The a-values were evaluated from the radiation transport calculation using the PHITS code. We examined the a-values by considering two kinds of radiation permeability effects seen in the mixer-settler system. The first effect is the escape of radiation energy from the mixer-settler system, which primarily occurs with gamma radiation and high-energy beta radiation. The geometry of the mixer-settler apparatus was modeled in the PHITS calculations to assess this effect for all radiations emitted by each nuclide. The second effect involves the distribution of radiation energy within the mixture. We employed a droplet model[14)] to represent the emulsion formed in the mixture. In this model, we focused on a single spherical oil droplet, assumed to have a diameter of 100 μm, to calculate the dose absorbed by the extraction solvent. For this droplet size, gamma and beta radiation deposited the energy uniformly into both the aqueous and organic phases of the mixture. In contrast, a portion of the energy from alpha-radiation emitted by alpha-emitting nuclides within the droplet escapes. Conversely, the droplet can also absorb energy from alpha radiation originating from the aqueous or organic phases outside it. The fraction of the dose absorbed in the extraction solvent in the mixture was evaluated using PHITS code with the droplet model to reflect the a-values in the mixer part. Details on the calculation procedure for the dose evaluation are described in our previous paper.[14)]

3. Experimental

To obtain the dose-dependent distribution ratios for the constituents, batch extraction experiment was performed using gamma-irradiated TDdDGA process solvents. The irradiation of the process solvents was carried out by using a ^{60}Co gamma source. The samples were irradiated for 16 hours at seven different dose rate points (0.3–6 kGy/h) The irradiated samples were the process solvent in contact with the aqueous solution of 1.5 mol/dm^3 HNO_3, 0.02 mol/dm^3 HEDTA, and 0.1 mol/dm^3 H_2O_2 (feed solution without metal ions), or 0.02 M HNO_3 aqueous solution (strip solution). Dosimetry was performed using the dichromate dosimeter [15)] and the dose rate was measured by irradiation for 1 hour at the same point. It is noted that the dose values described here are the water-equivalent.

The batch extraction was conducted as follows: The irradiated samples were once divided into each phase; A small amount of aqueous solution containing tracer metal ions representing the constituents was spiked into the irradiated aqueous phase; Equal volumes of the aqueous and organic phases were re-contacted and agitated for 10 minutes and then centrifuged for 3 minutes for phase separation. The concentrations of the non-radioactive elements in the aqueous phase were measured using an inductively coupled plasma mass spectrometer (7500, Agilent), and the distribution ratios were obtained from the concentrations in the aqueous phase before and after extraction. For ^{241}Am and ^{154}Eu, the concentrations of radionuclides in each phase were measured as radioactivity using a gamma-ray counter with a germanium detector (LO-AX 51,370/20-P, ORTEC). For ^{244}Cm, an alpha-radiation counter with a silicon semiconductor detector (Alpha Ensemble, SEIKO EG&G) was used. The distribution ratios were obtained as the ratio of the radioactivity in the organic phase to the aqueous phase.

III. Results and Discussion

1. Dose-Dependent Distribution Ratio

In the batch extraction experiments, no third phase was observed even for irradiated samples up to ~100 kGy. **Fig. 2** shows the absorbed dose dependence on distribution ratios (D) of selected metal ions, representing the radionuclides listed in Table 1. The D-values for actinide and rare-earth

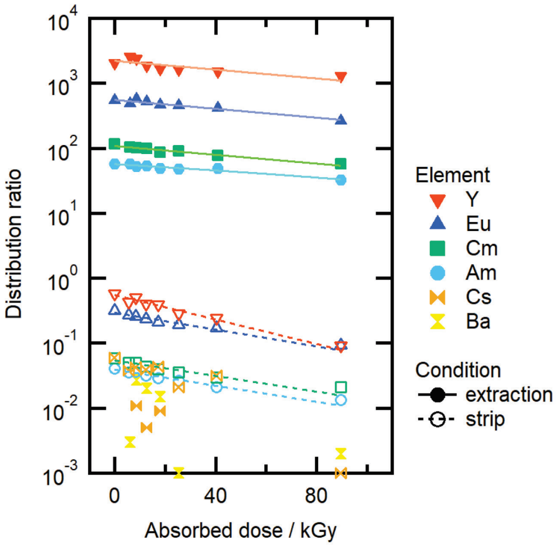

Fig. 2 Absorbed dose dependence on distribution ratios for extraction condition (closed symbol and solid line) and strip condition (open symbol and dashed line). Each symbol represents the observation result, and each line represents the fitting result.

elements decreased with increasing the absorbed dose for both extraction and strip conditions due to the radiolysis of the extractant. The *D*-values were fitted by single-exponential curves, as shown in Fig. 2, and the fitting results were used in the process simulation. Cs, Ba, and Sr were scarcely extracted, and no appreciable increase in *D*-value was observed for these metal ions even after irradiation, despite our initial concerns that the radiolytic degradation products could act as extractants for these non-target elements. Therefore, the migration of these three nuclides to the organic phase was disregarded in the simulation.

2. TDdDGA Process Simulation

For the simulated case shown in Fig. 1, extraction equilibrium was once achieved several hours after the beginning of the process operation, and the distribution of the constituents was not affected by the radiolysis effect in this time domain. **Fig. 3** shows dose rates in the organic phase for each stage of the mixing part after the extraction equilibrium. The calculated dose rate was 12.1 Gy/h as an average of the whole process, and the local highest dose rate was in the 6th stage (151 Gy/h for the mixing part and 195 Gy/h for the settling part) where the feed solution flows into the system. The dose rate in the 6th stage was decomposed into contributions from individual radionuclides and the result is shown in **Table 2**. The main radionuclides were MA and ^{90}Y. Since MA and ^{90}Y were extracted by TDdDGA, the energy deposition from these nuclides to the organic phase continued until they were stripped out into the aqueous phase. Conversely, ^{137}Cs, ^{137m}Ba, and ^{90}Sr were not extracted, but they contributed to the dose in the mixing part of extraction stages (1st–6th stages) because they remained in the aqueous phase.

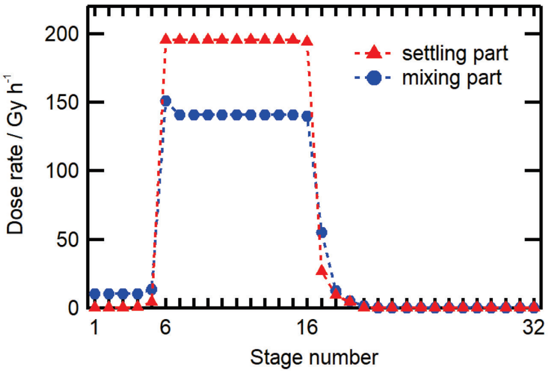

Fig. 3 Dose rates absorbed by the organic phase in each stage mixing part (blue circle) and settling part (red triangle) after 30 hours from the start of process operation. The dashed lines are just for eye-guide.

Figure 4 shows the time-dependent Am concentration in the strip solution at the outlet of the 17th stage (fraction). The plateau in Am concentration at 400 μmol/dm^3 indicates that the extraction process has reached equilibrium. Throughout the experimentally tested absorbed dose range of up to 90 kGy, as shown by the solid line until 7,500 hours in Fig. 4, no radiolytic degradation in the Am extraction was observed.

Table 2 The radionuclide breakdown of the dose rates in the 6th stage after 30 hours from the start of process operation.

Nuclide	Absorbed dose rate / Gy h^{-1}	
	Mixing part	Settling part
^{90}Sr	2.55	0.0198
^{90}Y	21.1	46.1
^{137}Cs + ^{137m}Ba	7.83	0.183
^{154}Eu	0.264	0.584
^{238}Pu	10.2	12.7
^{241}Am	39.6	47.6
^{244}Cm	69.5	88.2
total	151	195

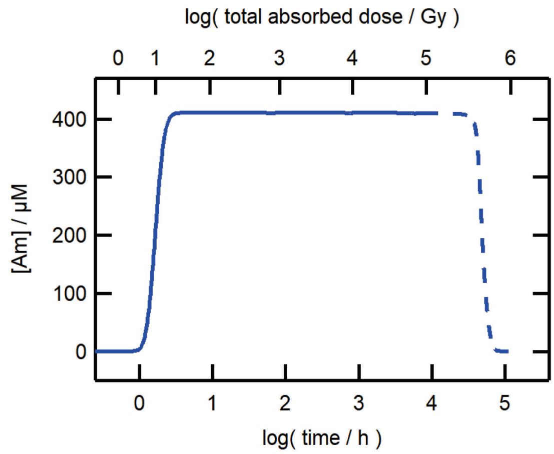

Fig. 4 Americium concentration in the strip solution at the outlet of the 17th stage (fraction) as functions of time (bottom) and total absorbed dose (top). The solid line indicates experimentally tested absorbed dose range, while the dashed line was obtained from the exploration of dose-dependent *D*-values.

The dashed line shown in Fig. 4 represents the predicted Am concentration after 7,500 hours based on an extrapolation of the fitted exponential decay of the *D*-values. This prediction suggests a decline in Am concentration due to radiolysis after 40,000 hours of process operation. The total absorbed dose in the extraction solvent reached approximately 600 kGy when the process degraded, corresponding to the dose at which the *D*-value for Am dropped to 1, as indicated by the fitted exponential decay observed in the batch experiment. This decline indicates a limitation in processing Am.

The total amount of Am recovered at the outlet of the strip solution was 711 g, calculated by integrating the time-dependent concentration in the solution with the flow rate of 145 cm^3/h until the concentration nearly reached zero, approximately after 80,000 hours. It should be noted that this simulation assumed the continuous recycling of the extraction solvent without any replacement or regeneration. Consequently, this amount of recovered Am represents the maximum recoverable amount for a specific volume of the extraction solvent, which is 2910 cm^3, and is limited by radiation-induced degradation. This finding underscores the importance of replacing and regenerating solvents.

The simulation methodology includes several approximations and assumptions. Negating the stage efficiency degradation or the physical property change (e.g., viscosity) due to radiolysis may cause an overestimation of the radiation-limited maximum recoverable amount for the extraction solvent. However, our approach proposed in this study is relatively easy to perform compared to completing all radiation-chemical reaction parameters, such as *G*-values and reaction rate constants, and elucidating their impact on extraction. This methodology could be suitable as a simple radiation stability evaluation from the viewpoint of MA separation process development.

IV. Conclusion

A simple model of the radiation-induced degradation of extraction performance was incorporated into the mass-balance differential equation for a multistage counter-current mixer-settler extraction process. In our calculation method, the radiolysis effect was formulated by using the dose-dependent *D*-values. We applied our method for the TDdDGA process. The dose-dependent *D*-values of the TDdDGA process solvent were determined from the gamma-ray irradiation experiment, and it was found that the *D*-values for MA and Y decrease exponentially with the absorbed dose. The *D*-value decay suggests a limitation of processing MA. Our process simulation is capable to incorporate the radiolytic degradation in extraction performance and provided an estimation for the radiation-limited maximum recoverable amount of MA in the TDdDGA process. Our proposed methodology offers a practical alternative to the detailed approaches, which are still difficult to implement due to a lack of necessary G-values and radiation-chemical reaction rate constants datasets. This approach enables a simplified but realistic evaluation of the radiation stability of the solvent extraction process, making it possible for early-stage process design and screening.

Acknowledgment

The gamma-irradiation experiment was conducted at Co-60 Irradiation Facilities in Takasaki Institute for Advanced Quantum Science (QST). We would like to thank T. Kurosawa and M. Shibata in JAEA for their support on batch extraction experiments.

References

1) B. J. Mincher, G. Modolo, S. P. Mezyk, “The Effects of Radiation Chemistry on Solvent Extraction 3: A Review of Actinide and Lanthanide Extraction,” *Solvent Extr. Ion Exch.*, **27**[5-6], 579-606 (2009).
2) J. Ravi, B. R. Selvan, K. A. Venkatesan, M. P. Antony, T. G. Srinivasan, P. R. V. Rao, “Radiolytic stability of di-2-ethylhexyl-dioctyl diglycolamide,” *Radiochim. Acta.*, **102**[5], 451-457 (2014).
3) D. Peterman, A. Geist, B. Mincher, G. Modolo, M. H. Galan, L. Olson, R. McDowell, “Performance of an *i*-SANEX System Based on a Water-Soluble BTP under Continuous Irradiation in a γ-Radiolysis Test Loop,” *Ind. Eng. Chem. Res.*, **55**[39], 10427-10435 (2016).
4) Y. Sugo, Y. Izumi, Y. Yoshida, S. Nishijima, Y. Sasaki, T. Kimura, T. Sekine, H. Kudo, “Influence of diluent on radiolysis of amides in organic solution” *Radiat. Phys. Chem.*, **76**[5], 794-800 (2007).
5) Y. Sugo, Y. Sasaki, M. Taguchi, N. S. Ishioka, “α-Radiation effect on solvent extraction of minor actinide,” *J. Radioanal. Nucl. Chem.*, **303**, 1381-1384 (2015).
6) C. A. Zarzana, G. S. Groenewold, B. J. Mincher, S. P. Mezyk, A. Wilden, H. Schmidt, G. Modolo, J. F. Wishart, A. R. Cook, “Comparison of the γ-Radiolysis of TODGA and T(EH)DGA Using UHPLC-ESI-MS Analysis,” *Solvent Extr. Ion Exch.*, **33**[5], 431-447 (2015).
7) G, P. Horne, C. A. Zarzana, C. Rae, A. R. Cook, S. P. Mezyk, P. R. Zalupski, A. Wilden, B. J. Mincher, “Does addition of 1-octanol as a phase modifier provide radical scavenging radioprotection for *N,N,N',N'*-tetraoctyldiglycolamide (TODGA)?” *Phys. Chem. Chem. Phys.*, **22**, 24978-24985 (2020).
8) Y. Ban, H. Suzuki, S. Hotoku, T. Kawasaki, H. Sagawa, N. Tsutsui, T. Matsumura, “Extraction of Trivalent Rare Earths and Minor Actinides from Nitric Acid with *N,N,N’,N’*-Tetradodecyldiglycolamide (TDdDGA) by Using Mixer-Settler Extractors in a Hot Cell,” *Solvent Extr. Ion Exch.*, **37**[1], 27-37 (2019).
9) Y. Ban, H. Suzuki, S. Hotoku, N. Tsutsui, Y. Tsubata, T. Matsumura, “Minor actinides separation by *N,N,N',N',N'',N''*-hexaoctyl nitrilotriacetamide (HONTA) using mixer-settler extractors in a hot cell,” *Solvent Extr. Ion Exch.*, **37**[7], 489-499 (2019)
10) H. Suzuki, Y. Tsubata, T. Kurosawa, M. Shibata, T. Kawasaki, S. Urabe, T. Matsumura, “Highly practical and simple ligand for separation of Am(III) and Eu(III) from highly acidic media,” *Anal. Sci.,* **32**[4], 477-479 (2016)
11) T. Shimogouchi, H. Naganawa, T. Nagano, B. Grambow, Y. Nagame, “Size Distribution of Droplets in Two Liquid-phase Mixture Compared between Liquid Spraying and Mechanical Stirring,”*Anal. Sci.,* **35**, 955-960 (2019)
12) Y. Tsubata, T. Asakura, Y. Morita, *Development of a Computer Code, PARC, for Simulation of Liquid-Liquid Extraction Process in Reprocessing*, JAEA-Data/Code 2008-010, Japan Atomic Energy Agency (2008).
13) T. Sato, Y. Iwamoto, S. Hashimoto, T. Ogawa, T. Furuta, S. Abe, T. Kai, Y. Matsuya, N. Matsuda, Y. Hirata, T. Sekikawa, L. Yao, P.E. Tsai, H.N. Ratliff, H. Iwase, Y. Sakaki, K. Sugihara, N. Shigyo, L. Sihver, K. Niita, “Recent improvements of the Particle and Heavy Ion Transport code System - PHITS version 3.33,” *J. Nucl. Sci. Technol.,* **61**[1], 127-135 (2024).
14) T. Toigawa, Y. Tsubata, T. Kai, T. Furuta, Y. Kumagai, T. Matsumura, “Re-evaluation of Radiation-Energy Transfer to an Extraction Solvent in a Minor-Actinide-Separation Process Based on Consideration of Radiation Permeability,” *Solvent Extr. Ion Exch.*, **39**[1], 74-89 (2021).
15) P. H. G. Sharpe, J. H. Barrett, A. M. Berkley, “Acidic aqueous dichromate solutions as reference dosimeters in the 10–40 kGy range”, *Int. J. Appl. Isot.*, **36**[8], 647-652 (1985)